Turkish Journal of Electrical Engineering & Computer Sciences

http://journals.tubitak.gov.tr/elektrik/

Research Article

Turk J Elec Eng & Comp Sci
(2013) 21: 360 – 372

doi:10.3906/elk-1112-14

Solution of transient stability-constrained optimal power flow using artificial bee colony algorithm

Kürşat AYAN[1], **Ulaş KILIÇ**[2,*]

[1]Department of Computer Engineering, Faculty of Computer and Information Science, Sakarya University, Adapazarı, Sakarya, Turkey

[2]Department of Electricity, Bucak Emin Gülmez Technical Vocational School, Mehmet Akif Ersoy University, Bucak, Burdur, Turkey

Received: 05.12.2011 • **Accepted:** 22.02.2012 • **Published Online:** 22.03.2013 • **Printed:** 22.04.2013

Abstract: The transient stability constraint should be taken into consideration for the solution of the optimization problems in power systems. This paper presents a solution for the transient stability-constrained optimal power flow (TSCOPF) by a novel approach based on the artificial bee colony algorithm. The formulas of TSCOPF are derived through the addition of rotor angle inequality constraints into optimal power flow relationships. In this nonlinear optimization problem, the objective function is taken into consideration as the fuel cost of the system. The proposed approach is tested on both a WSCC 3-generator, 9-bus system and a IEEE 30-bus system, and the test results obtained are compared to prove the efficiency and effectiveness of the approach with other approaches in the literature.

Key words: Artificial bee colony algorithm, constrained optimization, optimal power flow, power system, transient stability

1. Introduction

The optimal power flow (OPF) problem can be defined as meeting customers' energy needs with the minimum cost of energy production. This problem has become more important due to the increasing energy needs of customers day by day. Many numerical methods are used for solving the problem in the literature. Nonlinear programming [1], quadratic programming [2], Newton-based techniques [3], and linear programming [4] can be shown as examples of these methods. There are some certain disadvantages of using numerical methods in solving this problem. The most important of these are easy donning for the local minimum and starting point problems. Today, heuristic methods are used to eliminate these disadvantages. The biggest advantage of heuristic methods is that they can obtain global minimum or optimal solutions close to the global minimum in a short time. The genetic algorithm (GA) [5], particle swarm optimization (PSO) [6], ant colony algorithm (ACA) [7], differential evolution (DE) [8], and evolutionary programming (EP) [9] are examples of heuristic methods.

There are some limitations in the basic OPF problem: equality constraints and inequality constraints in spite of the power flow equations, and the restrictions inherent in the energy system. Today, the problems of energy systems have made it necessary for system designers to expand the OPF with different restrictions. Security constraint [10,11], the harmonic constraint [12,13], voltage stability constraint [14], and the transient stability constraint [15–17] can be given as examples of restrictions on the issue.

*Correspondence: ulaskilic@mehmetakif.edu.tr

The stability of power systems can be defined as reaching a new equilibrium point within certain limitations after exposure to the distorting effects of a system running at steady state. In stability calculations, the behavior of the system before, during, and after the disturbance effect is examined. What is expected from the system to be designed by the designers is that the system synchronism should not be disturbed, even after both a small and a large disturbance. With prompt switching of the defective lines as a result of a defective effect, the whole system will continue to work in a synchronized manner in the new state of equilibrium so that the customers will not have a cut in electricity. The temporary state of the stability constraint is obtained by including the new working conditions of the system, which will occur after failure, into the OPF problem with each being a constraint power.

The transient stability constraint OPF (TSCOPF) problem was solved with a control system in [17], where the method presented was tested for 2 different power systems in 4 different fault conditions. In [18], the TSCOPF problem was solved using the DE algorithm and the method presented was tested for 3 different power systems in 5 different fault conditions. For the solution of this problem in [19], EP was used along with fuzzy logic. The method proposed in this study, on the other hand, has been tested for different fault states in the IEEE 30-bus test system.

The conventional optimization techniques, which are used for both OPF and TSCOPF, are very sensitive to initial conditions. Sometimes these techniques are able to converge to local optimum solutions. In some cases, they are not able to converge to any solution. These troubles are overcome by new population-based heuristic optimization methods. These methods are PSO [15], the GA [20], DE [18], and the artificial bee colony (ABC) [21] algorithm. The ABC algorithm was proposed by Derviş Karaboğa. Recently, successful applications of the ABC algorithm to power systems have attracted attention [22–24] because the ABC algorithm is an efficient, effective, and fast algorithm for determining the global minimum points of nonlinear and nonconvex problems, such as the OPF and TSCOPF problems.

In this paper, the ABC algorithm is successfully applied to the TSCOPF problem for the first time. The detailed formulas of the TSCOPF problem are given in Section 2. The details of the ABC algorithm are explained in Section 3. The effectiveness and efficiencies of the ABC algorithm that is used for solving the TSCOPF problem are tested on 2 power systems, the WSCC 3-generator, 9-bus system and the IEEE 30-bus test system, as given in Section 4. Conclusions and discussion related to simulation results are given in Section 5.

2. TSCOPF formulation

2.1. OPF formulation

The OPF problem is an optimization problem whose mathematical equations are well known, and it is defined as follows:

Minimize the function of

$$f(x,u),$$

such that:

$$g(x,u)=0, \tag{1}$$

$$h(x,u)\leq 0.$$

In this study, the objective function $f(x,u)$ is taken as the total fuel cost, the equality constraints $g(x,u)$ are taken as the power flow equations, and the inequality constraints $h(x,u)$ are taken as transmission line limits and other security limits. Vectors x and u, the parameters of these functions, are called the state variable

vector and control variable vector, respectively. The state variable vector x is given as follows:

$$x^T = [P_{slack}, V_L, Q_g], \tag{2}$$

where the state variable vector x includes the slack bus active power, load bus voltage magnitude V_L, and generator reactive power Q_g. In that case, the control variable vector u is given as follows:

$$u^T = [P_g, V_g, T, Q_c], \tag{3}$$

where the control variable vector u consists of the active power generation except for the slack bus P_g, generator terminal voltage magnitude V_g, transformer tap ratio T, and reactive power generation or absorption of the compensation devices, such as the capacitor and reactor banks Q_c, respectively.

2.2. Objective function

The objective function is expressed as the total fuel cost of the entire power system with the fuel cost curve approximated as a quadratic function of the generator active power output.

$$f_i = \sum_{i=1}^{N_g} \left(a_i + b_i P_{gi} + c_i P_{gi}^2\right) \tag{4}$$

Here, f_i represents the total fuel cost, N_g represents the total number of generators, P_{gi} represents the active power generation of the i^{th} generator, and finally, a_i, b_i, and c_i represent the fuel cost coefficients of the i^{th} generator, respectively.

2.3. Equality constraints

The equalities in the OPF are defined as equality constraints:

$$P_{gi} - P_{li} - V_i \sum_{j=1}^{N} V_j (G_{ij} \cos\theta_{ij} + B_{ij} \sin\theta_{ij}) = 0 \qquad i = 1, ..., N, \tag{5}$$

$$Q_{gi} + Q_{ci} - Q_{li} - V_i \sum_{j=1}^{N} V_j \left(G_{ij} \sin\theta_{ij} - B_{ij} \cos\theta_{ij}\right) = 0 \qquad i = 1, ..., N, \tag{6}$$

where N is the total number of system buses, P_{li} is the active load of the i^{th} bus, Q_{li} is the reactive load of the i^{th} bus, Q_{gi} is the reactive power generation of the i^{th} bus, V_i is the voltage magnitude of the i^{th} bus, G_{ij} is the transfer conductance between bus i and j, B_{ij} is the transfer susceptance between bus i and j, and θ_{ij} is the voltage angle difference between bus i and j.

2.4. Inequality constraints

Active power outputs, reactive power outputs, and generation bus voltages are restricted by their lower and upper limits, and the generator constraints are given as follows:

$$P_{gi}^{\min} \le P_{gi} \le P_{gi}^{\max} \qquad i = 1, ..., N_g, \tag{7}$$

$$Q_{gi}^{\min} \le Q_{gi} \le Q_{gi}^{\max} \qquad i = 1, ..., N_g, \tag{8}$$

$$V_i^{\min} \le V_i \le V_i^{\max} \qquad i = 1, ..., N, \tag{9}$$

where $P_{gi}^{\min}$, $P_{gi}^{\max}$, $Q_{gi}^{\min}$, $Q_{gi}^{\max}$, $V_i^{\min}$, and $V_i^{\max}$ are the lower and upper limits of the variables, respectively. Transformer tap settings are restricted by their lower and upper limits, and the transformer constraints are given as follows:

$$T_i^{\min} \le T_i \le T_i^{\max} \qquad i = 1, ..., N_T, \tag{10}$$

where N_T is the total number of transformers and $T_i^{\min}$ and $T_i^{\max}$ are lower and upper limits of the corresponding variables, respectively. The shunt volt-ampere reactive (VAR) compensations are restricted by their limits and then the shunt VAR constraints are given as follows:

$$Q_{ci}^{\min} \le Q_{ci} \le Q_{ci}^{\max} \qquad i = 1, ..., N_c, \tag{11}$$

where N_c is the total number of compensator devices. $Q_{ci}^{\min}$ and $Q_{ci}^{\max}$ are the lower and upper limits of the corresponding variables, respectively.

2.5. Transient stability constraints

In a power system, the transient stability problem is explained through a range of algebraic equations shown in Eq. (12). The oscillation equations of i^{th} generator are:

$$\begin{aligned} &\dot{\delta}_i = \omega_i - \omega_0 \\ &M_i\dot{\omega}_i = \omega_0 \left(P_{mi} - P_{ei} - D_i\omega_i\right) \end{aligned} \qquad i = 1, ..., N_g, \tag{12}$$

where δ_i is the rotor angle of the i^{th} generator, ω_i is the rotor speed of the i^{th} generator, M_i is the moment of inertia of the i^{th} generator, D_i is the damping constant of the i^{th} generator, P_{mi} is the mechanical input power of the i^{th} generator, P_{ei} is the electrical output power of the i^{th} generator, and ω_0 is the synchronous speed.

Furthermore, the position of the center of inertia (COI) is defined as follows:

$$\delta_{COI} = \frac{\sum_{i=1}^{N_g} M_i\delta_i}{\sum_{i=1}^{N_g} M_i}. \tag{13}$$

A simplified criterion for the transient stability is expressed as the rotor angle deviation with respect to the COI, and hence the inequality constraints of the transient stability are formulated as follows:

$$\left|\delta_i - \delta_{COI}\right|_{\max} \le \delta_{\max} \qquad i = 1, .., N_g, \tag{14}$$

where $\left|\delta_i - \delta_{COI}\right|_{\max}$ represents the maximum deviation of the i^{th} generator rotor angle from the COI and $\delta_{\max}$ is the maximum rotor angle that is allowed, and its value is commonly based on experiences. The value of $\delta_{\max}$ is determined by the method of trial and error for both test systems in this study. These values are different for each system in the literature.

2.6. The calculation of fitness value

The state variables of the Newton–Raphson method are chosen as the control variables of the ABC algorithm and the control variables of the Newton–Raphson method are chosen as the state variables of the ABC algorithm. Thus, the fitness value of the individual is calculated by adding the violation at the control variables to the fuel cost determined as the result of the Newton–Raphson algorithm. As a result, the fitness value of each bee for the ABC algorithm can be formulated as follows:

$$\begin{aligned} f(x,u) &= f_i + K_V \sum_{i=1}^{N_{PQ}} \left(V_i - V_i^{\lim}\right)^2 + K_Q \sum_{i=1}^{N_g} \left(Q_{gi} - Q_{gi}^{\lim}\right)^2 + K_P \left(P_{slack} - P_{slack}^{\lim}\right)^2 \\ &+ K_T \sum_{i=1}^{N_g} \left(|\delta_i - \delta_{COI}|_{\max} - \delta^{\lim}\right)^2. \end{aligned} \tag{15}$$

$V_i^{\lim}$, $Q_{gi}^{\lim}$, $P_{slack}^{\lim}$, and $\delta_i^{\lim}$ are defined as follows:

$$V_i^{\lim} = \begin{cases} V_i^{\max}; V_i > V_i^{\max} \\ V_i^{\min}; V_i < V_i^{\min} \end{cases}, \tag{16}$$

$$Q_{gi}^{\lim} = \begin{cases} Q_{gi}^{\max}; Q_{gi} > Q_{gi}^{\max} \\ Q_{gi}^{\min}; Q_{gi} < Q_{gi}^{\min} \end{cases}, \tag{17}$$

$$P_{slack}^{\lim} = \begin{cases} P_{slack}^{\max}; P_{slack} > P_{slack}^{\max} \\ P_{slack}^{\min}; P_{slack} < P_{slack}^{\min} \end{cases}, \tag{18}$$

$$\delta_i^{\lim} = \begin{cases} \delta_{\max}; |\delta_i - \delta_{COI}|_{\max} > \delta_{\max} \\ 0; |\delta_i - \delta_{COI}|_{\max} < \delta_{\max} \end{cases}, \tag{19}$$

where $f(x,u)$ shows the fitness function; N_{PQ} shows the number of load buses; $P_{slack}^{\lim}$, $V_i^{\lim}$, and $Q_{gi}^{\lim}$ denote the violated upper or lower limits of the related variables; and K_P, K_Q, K_V, and K_T are the penalty weights of the active power output of the slack bus, reactive power output of the generator bus, load bus voltage magnitude, and transient stability limit, respectively. If the constraints are between their upper limits and lower limits, then the related penalty value is assumed as zero.

3. Artificial bee colony algorithm

The ABC algorithm has been successfully applied in different fields of science such as computer-industrial engineering, hydraulic engineering, mechanical engineering, and electronic engineering since 2005 [25–28].

The ABC algorithm is a population-based algorithm that was inspired by bees looking for food, and the flow chart of this is shown in Figure 1. This algorithm is divided into 2 groups consisting of worker bees and nonworker bees. Nonworker bees consist of onlooker bees and scout bees.

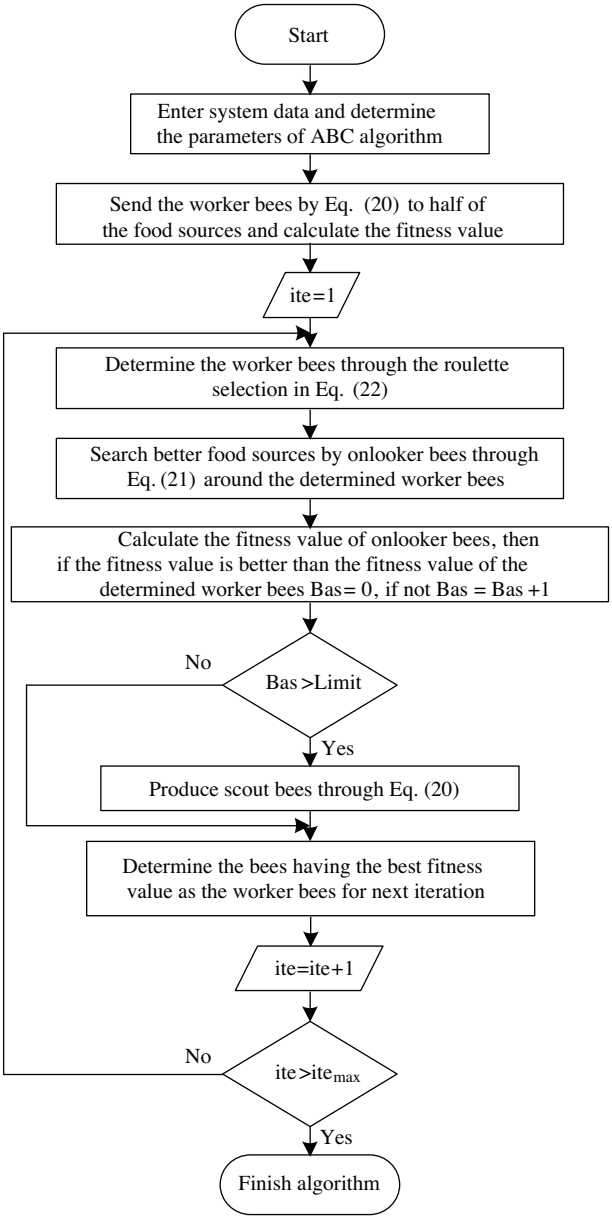

Figure 1. Flowchart of the ABC algorithm.

Inside the algorithm, all of the worker bees are sent to half of the food. After the calculation of the food amount in this source, a local search is implemented around the food by the onlooker bees. If another source that has more nutrition is explored, this source is updated as a new food source. If a better food source could not be found by the onlooker bees or the scout bees following a certain cycle, the onlooker bees are oriented towards a random food source. Following each cycle, the bees in the population are sorted according to the food sources they find and the best bees are transferred to the next cycle. When the stopping criterion is ensured, the algorithm is ended. The initial points for the algorithm and the food sources that the worker bees will fly to are determined by Eq. (20):

$$u_{ij} = u_{\min j} + rand \times (u_{\max j} - u_{\min j},) \tag{20}$$

where the parameters $u_{\min j}$ and $u_{\max j}$ show the minimum and maximum of the variable u_j. After the initial

bee population is produced, the sources that the onlooker bees will fly to are determined by Eq. (21):

$$v_{ij} = \min(u_{ij}, u_{kj}) + (\max(u_{ij}, u_{kj}) - \min(u_{ij}, u_{kj})) \times (rand - 0.5) \times 2, \tag{21}$$

where v_{ij}, $\min(u_{ij}, u_{kj})$, and $\max(u_{ij}, u_{kj})$ represent the onlooker bee to be produced and the minimum and maximum of the variables of bees u_{ij} and u_{kj}, respectively. The $rand$ value is between 0 and 1. The food sources that the onlooker bees will settle at are determined by Eqs. (22) and (23). For the selection of the onlooker bees, roulette wheel selection [29] is utilized. In roulette wheel selection, the probability of the selection of the bee with high efficiency is higher. The efficiency of a bee within the population in roulette wheel selection is given in Eq. (22).

$$P_i = \frac{fit_i}{\sum_{j=1}^{NF} fit_j} \tag{22}$$

where fit_i and NF show the modified fitness value of the i^{th} solution and the number of the food sources, respectively. The term of fit_i is calculated by Eq. (23).

$$fit_i = \frac{1}{f_i}, \tag{23}$$

Worker bees whose sources have come to an end become scout bees and start to randomly search for new food source nectar, for example, by Eq. (20). There is no guidance for the scout bees when searching for new food sources. They primarily try to find any kind of food source. The worker bee whose food source nectar has come to an end or whose profitability of the food source drops under a certain level is selected and classified as the scout bee.

3.1. Simulation results

In this section, the ABC algorithm proposed for the solution of the TSCOPF problem is tested both on a WSCC 3-generator, 9-bus system and a IEEE 30-bus system. For both of the test systems, a classical generator model is used for the synchronous generators and a constant impedance model is used for the loads. The software developed with MATLAB is run with a Core 2 Duo 2.67 CPU and 1 GB RAM. The software used for the transient stability analysis was given in [30]. In this study, the transient stability analysis is applied to the whole bee population.

As in many studies in the literature, the ABC algorithm's stopping criterion is chosen as 100 iterations. The optimum results are obtained as 75 and 100 iterations for the WSCC 3-generator, 9-bus system and the IEEE 30-bus system, respectively. When the number of iterations grows too much ($>$1000 iterations), the algorithm obtains the global optimum for each attempt, but the time consumed increases, as well. For this reason, various attempts have been made for different population sizes in the number of chosen iterations. As a result of the trials of different population sizes, it was detected that the optimum conclusion is reached immediately with the sizes of 5 and 10 colonies for the WSCC 3-generator, 9-bus system and the IEEE 30-bus systems, respectively.

3.2. WSCC 3-generator, 9-bus system

The WSCC 3-generator, 9-bus system is shown in Figure 2 and the system data are given in [31]. The fuel cost coefficients are taken from [17]. The upper and lower limits of all of the generator voltage magnitudes are set at

1.10 p.u. and 1.00 p.u., respectively. The upper and lower limits of the voltage magnitudes of the other buses are also set at 1.10 p.u. and 0.90 p.u., respectively. For this test system, the OPF and TSCOPF problems are solved for 2 fault cases. The step time of the integration is 10 ms for the transient stability simulation and the simulation period is taken into consideration as 5.0 s. Here, $\delta_{\max}$ is set to 200° for the WSCC 3-generator, 9-bus system.

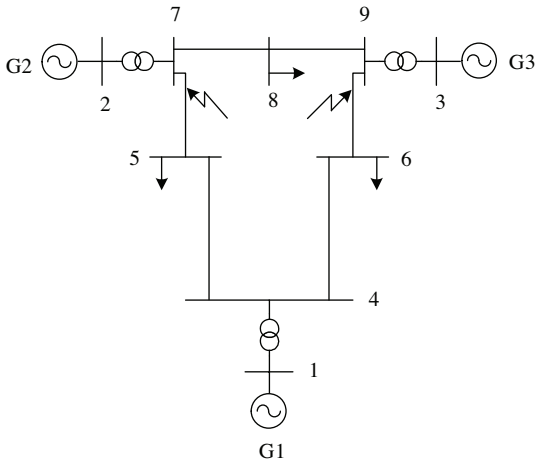

Figure 2. One-line diagram of the WSCC 3-generator, 9-bus system.

Base case: There is no transient stability constraint in this optimization problem. The objective in this optimization problem is to minimize the total fuel cost of the entire power system to subject the generator constraints.

The 2 fault cases for the test system are:

Case A: A 3-phase to ground fault at bus 7 and in line 7-5 in the system. The fault clearing time is taken as 0.35 s; this time is longer than the CCT of 0.162 s.

Case B: A 3-phase to ground fault at bus 9 and in line 9-6 in the system. The fault clearing time is taken as 0.3 s; this is longer than the CCT of 0.214 s.

For the base OPF, Case A and Case B and the minimum, maximum, and average fuel costs are given in Table 1. The small differences between the minimum and maximum solutions obtained for these 3 cases show that the proposed method is quite a strong algorithm in the determination of the global optimum. The results obtained by the ABC algorithm are compared to those of the DE method in [18], the trajectory sensitivities (TS) method in [17], and the time-domain simulations (TDS) method in [32], and all of the solutions are given in Table 2. For each of the 3 cases, it can be seen that lower fuel costs are obtained by the ABC algorithm. Although the number of variables is low and the searching area is small, the ABC algorithm has attained more successful solutions than those in the literature.

For each case, the variation of fuel cost against the iterations is shown in Figure 3. The weight of the total fuel cost in the fitness value rises such that the base case does not contain the transient stability constraint. Thus, as the iteration number rises, the total fuel cost falls. If the constraints are between their upper and lower limits, then the related penalty value is assumed as zero. If the transient stability constraint is added to the optimization problem, then the weight of the total fuel cost in the fitness value falls until the system remains stable. For case A, the total fuel cost fell after the proposed algorithm attained an optimum at 35 iterations. For case B, an optimum is attained at 10 iterations. Next, both of the systems remain stable and the total fuel cost is minimized.

Table 1. Test solutions for the WSCC 3-generator, 9-bus system.

Case	Base case	A	B
$P_{g1} + Q_{g1}$ (MVA)	107.15-j37.17	117.69-j65.51	121.23-j51.66
$P_{g2} + Q_{g2}$ (MVA)	114.18-j48.64	105.89-j41.88	120.63-j42.72
$P_{g3} + Q_{g3}$ (MVA)	96.74-j60.64	94.23-j56.83	75.94-j56.20
V_1 (p.u.)	1.033	1.025	1.019
V_2 (p.u.)	1.024	1.070	1.041
V_3 (p.u.)	1.028	1.070	1.044
Minimum cost ($/h)	1131.87	1133.18	1137.78
Maximum cost ($/h)	1132.22	1138.8	1146.7
Average cost ($/h)	1132.04	1135.9	1142.2

Table 2. Comparison of total fuel costs for the WSCC 3-generator, 9-bus system.

Case	DE [18]	TS [17]	TDS [32]	ABC
Base case ($/h)	1132.30	1132.59	1132.18	1131.87
Case A ($/h)	1140.06	1191.56	1134.01	1133.18
Case B ($/h)	1147.77	1179.95	1137.82	1137.78

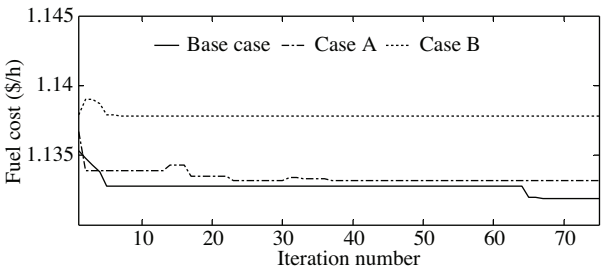

Figure 3. The fuel cost variation against the iterations for the WSCC 3-generator, 9-bus system.

The relative rotor angles for Cases A and B are shown in Figures 4 and 5, respectively. It can be seen clearly that the system still remains stable after the disturbance.

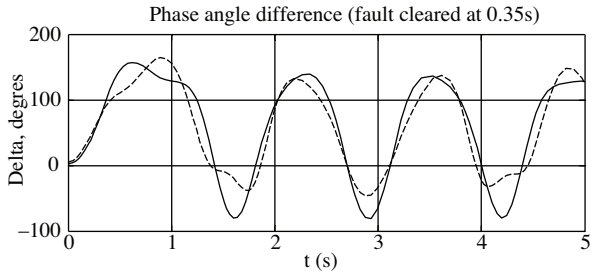

Figure 4. Relative rotor angles for the fault at bus 7.

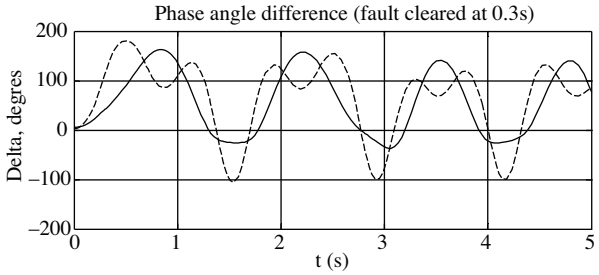

Figure 5. Relative rotor angles for the fault at bus 9.

3.3. IEEE 30-bus system

The IEEE 30-bus test system contains 41 transmission lines, 6 generators, and 4 transformers, as shown in Figure 6. The system data were taken from [33] and the data for the generators in the test system are given in Table 3. The total active load and reactive load of the system is 189.2 MW and 107.2 MVar, respectively. Here, $\delta_{\max}$ is set to 50° for the IEEE 30-bus system.

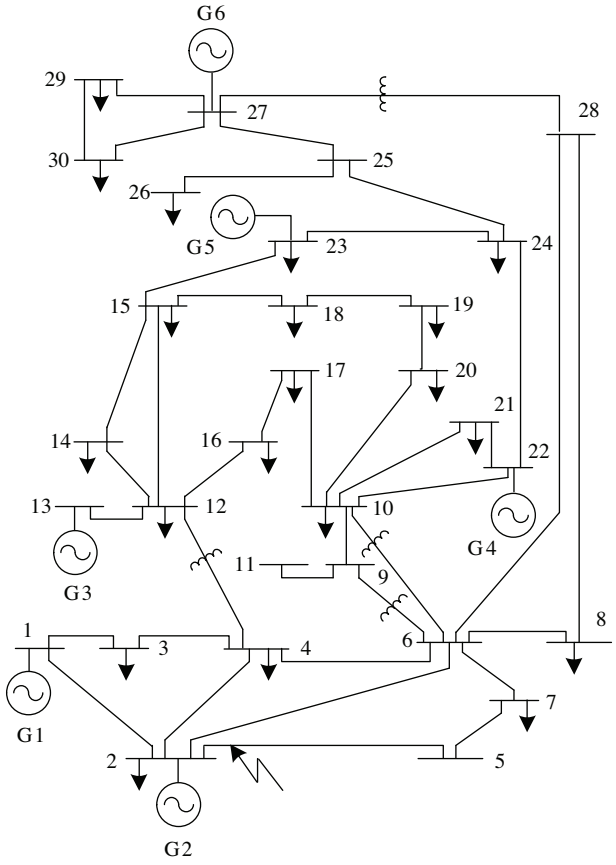

Figure 6. IEEE 30-bus system one-line diagram.

Table 3. Generator data for the IEEE 30-bus system.

Bus number	Active power limits		Cost coefficient		
	Min (MW)	Max (MW)	a	b	c
1	0	80	0.0000	2.00	0.02000
2	0	80	0.0000	1.75	0.01750
13	0	40	0.0000	3.00	0.02500
22	0	50	0.0000	1.00	0.06250
23	0	30	0.0000	3.00	0.02500
27	0	55	0.0000	3.25	0.00834

The following fault case is studied for the test system:

Case C: A 3-phase to ground fault at bus 2 and in line 2-5 in the system. The fault clearing time is taken as 0.18 s. The step time of the integration is at 10 ms for the transient stability simulation and the simulation period is taken into consideration as 5.0 s.

For the IEEE 30-bus test system, the fuel cost variation against the iterations is shown in Figure 7. Note that the total fuel cost tends to fall after the proposed algorithm attains an optimum at 10 iterations. The relative rotor angles are shown in Figure 8 for Case C. It can be seen from Figure 8 that all of the generators remain stable during the simulation period. The obtained solutions are compared with those in the literature and all of the solutions are given in Table 4. It can be seen from the results given in the Table 4 that the worst solution obtained by the ABC algorithm is better than the best solution obtained by the other algorithms. These

results prove the success of the ABC algorithm for solving the TSCOPF problem. For solving the TSCOPF problem, the ABC algorithm is faster than the GA by 77.1%, PSO by 70.1%, and EP incorporating neural network by 21.8%.

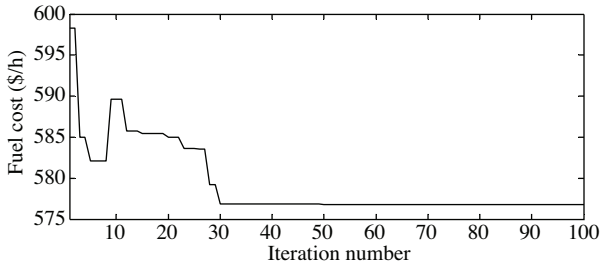

Figure 7. The fuel cost variation against the iterations for the IEEE 30-bus system.

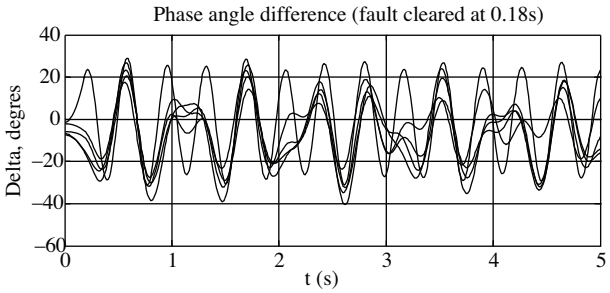

Figure 8. Relative rotor angles for the fault at bus 2.

Table 4. Comparison of all of the results for the IEEE 30-bus system.

Case C	GA [15]	PSO [15]	EPNN [19]	ABC
P_{g1} (MW)	41.88	43.63	48.95	42.65
P_{g2} (MW)	56.38	58.05	38.41	60.15
P_{g3} (MW)	22.94	23.29	23.34	17.96
P_{g4} (MW)	37.63	32.49	24.65	24.68
P_{g5} (MW)	16.7	17.04	17.61	15.00
P_{g6} (MW)	16.53	17.54	38.99	31.64
T_1 (buses 6–9)	1.01	1.01	1.01	1.0104
T_2 (buses 6–10)	0.95	0.96	0.98	1.0115
T_3 (buses 4–12)	1.00	1.01	1.03	0.9822
T_4 (buses 27 and 28)	0.97	0.97	1.04	0.9968
Best cost ($/h)	585.62	585.17	585.12	576.755
Worst cost ($/h)	585.71	585.69	586.73	581.980
Average cost ($/h)	585.66	585.34	585.84	579.367
Time (s)	752.3	576.4	220.17	172

4. Conclusions

In this paper, the ABC algorithm is successfully applied for the solution to the TSCOPF problem for the first time. Here, 2 test systems and 3 fault cases are taken into consideration. For these cases, the TSCOPF problem is solved by the ABC algorithm. The solutions obtained by the ABC algorithm are compared with those obtained by other heuristic methods in the literature. According to this comparison, it can be clearly seen that the ABC algorithm is superior to other algorithms in terms of both the solution time and the fuel cost. Furthermore, the ABC algorithm reaches the global optimum quickly and effectively. These results show us that the ABC algorithm can be used to efficiently solve the TSCOPF problem of large power systems. It can be seen from the obtained optimization results that this algorithm, which was developed in recent years, can be applied to many problems in power systems.

References

[1] H. Habiabollahzadeh, G.X. Luo, A. Semlyen, "Hydrothermal optimal power flow based on a combined linear and nonlinear programming methodology", IEEE Transactions on Power Systems, Vol. 4, pp. 530–537, 1989.

[2] J.S. Lipowski, C. Charalambous, "Solution of optimal load flow problem by modified recursive quadratic programming method", IEE Proceedings - Generation, Transmission and Distribution, Vol. 128, pp. 288–294, 1981.

[3] S. Zhang, M.R. Irving, "Enhanced Newton-Raphson algorithm for normal, controlled and optimal power flow solutions using column exchange techniques", IEE Proceedings - Generation, Transmission and Distribution, Vol. 141, pp. 647–657, 1994.

[4] R. Mota-Palomino, V.H. Quintana, "Sparse reactive power scheduling by a penalty-function linear programming technique", IEEE Transactions on Power Systems, Vol. l, pp. 31–39, 1986.

[5] M.S. Osman, M.A. Abo-Sinna, A.A. Mousa, "A solution to the optimal power flow using genetic algorithm", Applied Mathematics and Computation, Vol. 155, pp. 291–405, 2004.

[6] S. He, J.Y. Wen, E. Prempain, Q.H. Wu, J. Fitch, S. Mann, "An improved particle swarm optimization for optimal power flow", International Conference on Power System Technology, Vol. 2, pp. 1633–1637, 2004.

[7] J.G. Vlachogiannis, N.D. Hatziargyriou, K.Y. Lee, "Ant colony system-based algorithm for constrained load flow problem", IEEE Transactions on Power Systems, Vol. 20, pp. 1241–1249, 2005.

[8] S. Sayah, K. Zehar, "Modified differential evolution algorithm for optimal power flow with non-smooth cost functions", Energy Conversion and Management, Vol. 49, pp. 3036–3042, 2008.

[9] Y.R. Sood, "Evolutionary programming based optimal power flow and its validation for deregulated power system analysis", International Journal of Electrical Power & Energy Systems, Vol. 29, pp. 65–75, 2007.

[10] P. Somasundaram, K. Kuppusamy, R.P. Kumudini Devi, "Evolutionary programming based security constrained optimal power flow", Electric Power Systems Research, Vol. 72, pp. 137–145, 2004.

[11] H. Vahedi, S.H. Hosseini, R. Noroozian, "Bacterial foraging algorithm for security constrained optimal power flow", 7th International Conference on the European Energy Market, pp. 1–6, 2010.

[12] Y.Y. Hong, "Optimal harmonic power flow", IEEE Transactions on Power Delivery, Vol. 12, pp. 1267–1274, 1997.

[13] I. Ziari, A. Jalilian, "Optimal harmonic power flow using an ant colony system-based algorithm", 43rd International Universities Power Engineering Conference, pp. 1–4, 2008.

[14] S. Kim, T.Y. Song, M.H. Jeong, B. Lee, Y.H. Moon, J.Y. Namkung, G. Jang, "Development of voltage stability constrained optimal power flow (VSCOPF)", Power Engineering Society Summer Meeting, Vol. 3. pp. 1664–1669, 2001.

[15] N. Mo, Z.Y. Zou, K.W. Chan, T.Y.G. Pong, "Transient stability constrained optimal power flow using particle swarm optimization", IET Generation, Transmission & Distribution, Vol. 1, pp. 476–483, 2007.

[16] A. Hoballah, I. Erlich, "PSO-ANN approach for transient stability constrained economic power generation", IEEE Bucharest Power Tech Conference, pp. 1–6, 2009.

[17] T.B. Nguyen, M.A. Pai, "Dynamic security-constrained rescheduling of power systems using trajectory sensitivities", IEEE Transactions on Power Systems, Vol. 18, pp. 848–854, 2003.

[18] H.R. Cai, C.Y. Chung, K.P. Wong, "Application of differential evolution algorithm for transient stability constrained optimal power flow", IEEE Transactions on Power Systems, Vol. 23, pp. 719–728, 2008.

[19] K. Tangpatiphan, A. Yokoyama, "Evolutionary programming incorporating neural network for transient stability constrained optimal power flow", Joint International Conference on Power System Technology and IEEE Power India Conference, pp. 1–8, 2008.

[20] K.Y. Chan, S.H. Ling, K.W. Chan, H.H.C. Iu, G.T.Y. Pong, "Solving multi-contingency transient stability constrained optimal power flow problems with an improved GA", IEEE Congress on Evolutionary Computation, pp. 2901–2908, 2007.

[21] D. Karaboga, "An idea based on honey bee swarm for numerical optimization", Technical Report-TR06, Erciyes University, Engineering Faculty, Computer Engineering Department, 2005.

[22] K. Ayan, U. Kılıç, "Solution of multi-objective optimal power flow with chaotic artificial bee colony algorithm", International Review of Electrical Engineering, Vol. 6, pp. 1365–1371, 2011.

[23] K. Ayan, U. Kılıç, "Comparison of GA, MA and ABC algorithm for solution of optimal power flow", 6th International Advanced Technologies Symposium, Vol. 3, pp. 13–18, 2011.

[24] T.L. Nguyen, Q.A. Nguyen, "Application artificial bee colony algorithm (ABC) for reconfiguring distribution network", 2nd International Conference on Computer Modeling and Simulation, pp. 102–106, 2010.

[25] Y. Marinakis, M. Marinaki, N. Matsatsinis, "A hybrid discrete artificial bee colony-GRASP algorithm for clustering", 39th International Conference on Computers and Industrial Engineering, pp. 548–553, 2009.

[26] F. Kang, J.J. Li, Q. Xu, "Hybrid simplex artificial bee colony algorithm and its application in material dynamic parameter back analysis of concrete dams", Journal of Hydraulic Engineering, Vol. 40, pp. 736–742, 2009.

[27] A.Ş. Şahin, B. Kılıç, U. Kılıç, "Design and economic optimization of shell and tube heat exchangers using artificial bee colony (ABC) algorithm", Energy Conversion and Management, Vol. 52, pp. 3356–3362, 2011.

[28] N. Karaboga, "A new design method based on artificial bee colony algorithm for digital IIR filters", Journal of the Franklin Institute, Vol. 346, pp. 328–348, 2009.

[29] Y. He, C. Jian, "Clonal selection algorithm with adaptive mutation and roulette wheel selection", Computational Intelligence and Security Workshops, pp. 93–96, 2007.

[30] Power System Toolbox Webpage, Rensselaer Polytechnic Institute, http://www.ecse.rpi.edu/pst/PST.html, 2011.

[31] P.W. Sauer, M.A. Pai, Power System Dynamics and Stability, Englewood Cliffs, New Jersey, Prentice Hall, 1998.

[32] R. Zarate-Minano, T. Van Cutsem, F. Milano, A.J. Conejo, "Securing transient stability using time-domain simulations within an optimal power flow", IEEE Transactions on Power Systems, Vol. 25, pp. 243–253, 2010.

[33] R. Zimmerman, D. Gan, MATPOWER: A MATLAB Power System Simulation Package, http://www.pserc.cornell.edu/matpower/, 2011.